

INTERFERENCE OF O $K\alpha$ GHOST FEATURES IN X-RAY-EXCITED AUGER SPECTRA*

B E KOEL** and J M WHITE

Department of Chemistry, University of Texas, Austin, Texas 78712 (U S A)

(First received 22 May 1980, in final form 15 September 1980)

ABSTRACT

We have noted the interference of O $K\alpha$ ghost peaks in spectra obtained using unmonochromatized X-ray sources, particularly in C(KVV) and O(KVV) X-ray-excited Auger spectra. The source of the undesirable O $K\alpha$ photons is a surface oxide on the Mg or Al anode of the polychromatic X-ray sources used. A calculation of the oxide thickness required to give the observed ghost intensity in measurements on a gold sample using a heavily oxidized Mg anode is given and the estimated oxide thickness found plausible. Since it may be impossible to operate the anode with no oxide present, the use of a standard Au sample is suggested as an excellent test for the presence of O $K\alpha$ X-radiation from unmonochromatized X-ray sources.

In the course of investigating chemisorbed carbon- and oxygen-containing species using X-ray-excited Auger spectroscopy (XAES) we have found features in the C(KVV) and O(KVV) regions which are not present to the same extent in electron-excited Auger spectra (EAES). In this paper we provide evidence that the difference in intensity of these features comes from an artifact, i.e., ghost photoelectron peaks due to the presence of O $K\alpha$ X-radiation from our polychromatic Mg X-ray source. We suggest that this same artifact is responsible for previously reported differences between X-ray- and electron-excited AES [1]. The purpose of this paper is to draw attention to the importance of considering such ghost features, particularly when measuring and analyzing relatively weak electron signals produced by polychromatic sources. In addition, we show that the use of a clean Au sample provides an excellent means for testing for the presence of the O $K\alpha$ ghost line and for calibrating the relative intensity of these ghost features.

Any X-ray source used without a monochromator delivers both bremsstrahlung and characteristic X-rays, the latter due to any material found in

* Supported in part by the Robert A. Welch Foundation

** Am. Chem. Soc. Proctor and Gamble Fellow

the near-surface region of the anode. Impurities such as oxygen in a Y Mg source [2], and anode construction materials such as copper [3] have been reported as contributors to undesirable characteristic radiation. Potentially, carbon could also be a contributor. Characteristic X-rays from contaminated sources contribute separate photoelectron peaks (ghosts) to XPS spectra because photoelectron kinetic energies are proportional to the photon energy used to produce the ionization. These ghost peaks can be mapped with respect to those derived from the Mg $K\alpha$ X-rays (principal peaks) using the constant-difference rule, the difference in photon energies is constant and equal to the difference in photoelectron kinetic energies. Wagner et al [4] give a useful tabulation of the displacements of ghost peaks for Mg and Al $K\alpha$ sources. O $K\alpha$ ($h\nu = 524.9$ eV) ghost peaks are displaced to lower kinetic energy by 728.7 and 961.7 eV respectively from the Mg $K\alpha$ ($h\nu = 1253.6$ eV) and Al $K\alpha$ ($h\nu = 1486.6$ eV) photoelectron peaks. On the Mg $K\alpha$ binding-energy (BE) scale, for example, O $K\alpha$ ghosts appear at 728.7 eV higher BE. While peak positions can be mapped readily, comparison of relative intensities is not possible directly, e.g. because of the different variation with photon energy of the photoionization cross-sections for various orbitals.

In our experiments, which utilized a Perkin-Elmer PHI Mg source, we observed an anomalously large and nearly constant-energy peak in the XAES C(KVV) spectra of condensed benzene, dimethyl ether, and methanol. In order to determine that this peak was an artifact and to measure accurately its intensity and position we used a spectrum of clean gold.

Figure 1 shows that the O $K\alpha$ ghost peaks from the Au 4*f* orbitals (BE

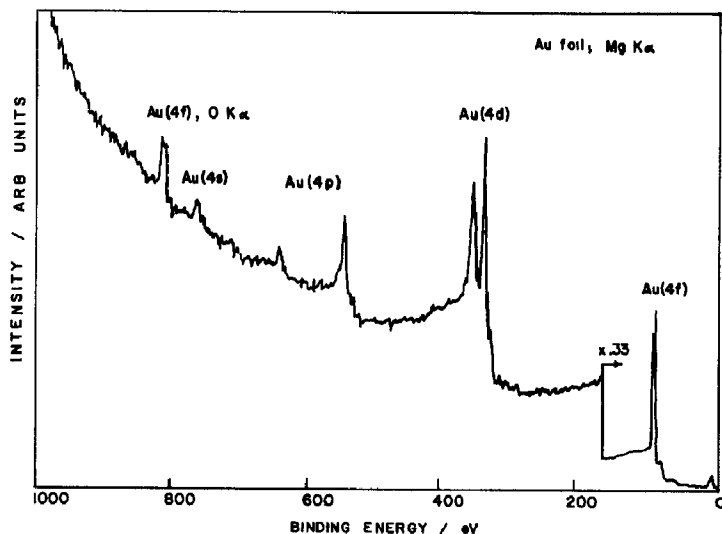


Fig 1 XPS spectrum of clean gold foil, obtained using an oxidized Mg anode. The impurity O $K\alpha$ X-radiation produces ghost photoelectron peaks with an apparent higher binding energy of 728.7 eV. The Au 4*f* O $K\alpha$ ghost peak is seen here.

83.8 and 87.4 eV) appear at 812.5 and 816.1 eV on the Mg $K\alpha$ BE scale and have an intensity $\sim 11\%$ of that of the principal peaks. This intensity is the largest we have observed, and was due to a highly oxidized Mg anode. We present below a discussion to account for this impurity intensity. Simply by replacing the $2\text{ }\mu\text{m}$ -thick Al window and mechanically polishing the anode of this source, the relative intensity of the ghost was reduced to $\sim 1.5\%$. However, further polishing or H_2 reduction in situ did not completely eliminate these ghosts. We also observed Au $4f$ O $K\alpha$ ghost peaks with a relative intensity of 6.5% from an Al source used routinely in this laboratory.

The observed XAES C(KVV) lineshape for condensed methyl ether, $(\text{CH}_3)_2\text{O}$, using an oxidized Mg anode, is shown in Fig 2 (curve A). The lineshape was found by subtracting the secondary-electron background [5] and deconvoluting the extrinsic losses and analyzer response from the raw data [6,7]. It contains an unusually intense peak at 236 eV, 1 eV at a KE 20 eV lower than the main peak at 256 eV. This sample was a very thick multilayer and some small, uniform energy correction may need to be applied for charging, although these results agree closely in energy with those found in ref. 1. The intense low-KE peak is primarily the O $K\alpha$ ghost of the

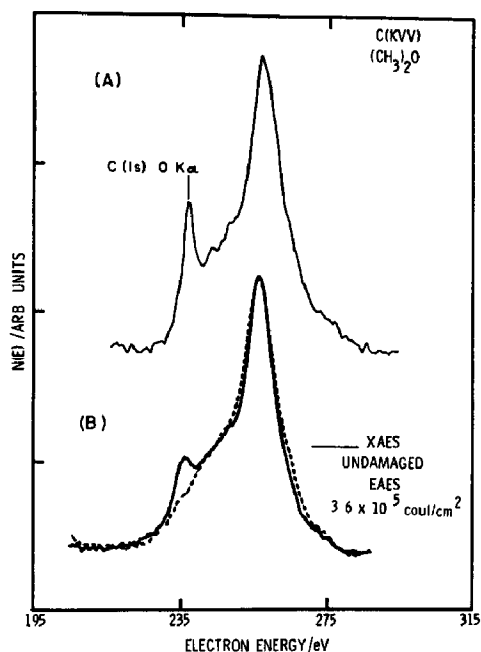


Fig 2 Curve A the observed XAES C(KVV) lineshape for a thick multilayer of $(\text{CH}_3)_2\text{O}$ after background subtraction and deconvolution to remove extrinsic losses and analyzer response. The spectrum was obtained using an oxidized Mg anode similar to that for Fig 1. The C 1s O $K\alpha$ ghost photoelectron peak contributes significant intensity at 20-eV lower kinetic energy than the peak in the C(KVV) lineshape. Curve B EAES and XAES C(KVV) spectra of $(\text{CH}_3)_2\text{O}$ multilayers after correcting for background and inelastic scattering processes (data from ref. 1).

C 1s photoelectron peak at KE 964.7 eV from Mg $K\alpha$ photons (the displacement of the ghost peak is 728.7 eV). The measured relative intensity of the ghost C 1s peak to the principal C 1s peak is $\sim 18\%$. Holloway et al [1] reported differences in the EAES and XAES C(KVV) lineshapes from condensed multilayers of methanol and methyl ether, primarily a peak at ~ 233 eV in the XAES C(KVV) spectra, at ~ 20 eV lower energy than the main peak. They pointed out that Jennison and co-workers' calculations [8] demonstrate that a feature at ~ 233 eV is a normal transition in the C(KVV) spectrum of methanol, and suggested that the enhancement of this peak in XAES was probably due to differences in the probability of shake-up or shake-off processes dependent upon the excitation mode. Figure 2 (curve B) also shows the XAES and EAES C(KVV) spectra for condensed methyl ether taken from ref 1. There is an excellent match in the displacement from the main peak between the obviously spurious peak in curve A and the enhanced feature in curve B. It seems clear, on the basis of our spectra, that the enhancement in the XAES spectrum of Fig 2 (curve B) is due to a small amount of contaminating O $K\alpha$ X-radiation producing a C 1s ghost peak at this energy. Unequivocal proof requires an experiment using a monochromatic source, but our Au results represent compelling evidence supporting our conclusion. Holloway et al [1] reported similar spectra with both Mg and Al sources. They inferred that impurity X-rays were not important, however, the relative O $K\alpha$ ghost intensities may have been similar for the two X-ray sources they used. In their work, assuming the enhancement is totally due to O $K\alpha$ photons, the measured intensity of the O $K\alpha$ C 1s ghost peak can be estimated to be $\sim 2\%$ of that of the Mg $K\alpha$ C 1s peak. This small O $K\alpha$ intensity is not unreasonable, consequently we expect electron and photon excitation to give the same C(KVV) lineshape for methyl ether.

Figure 3(a) shows the XAES O(KVV) spectra obtained for CO on Ni(100) at 200 K using an oxidized Mg anode. Obvious spurious structure exists in the O(KVV) region near 730 and 796 eV on the Mg BE scale. Figure 3(b) shows the near-valence region of Ni. The O $K\alpha$ ghosts of these peaks, which appear at 728.7 eV higher BE, add intensity in the O(KVV) spectra. The point to be made is that for weak O $K\alpha$ intensities the origin of the resultant ghost structure could easily be overlooked and incorrectly assigned.

It is of interest to consider how the level of oxygen impurity in the anode is related to the relative intensity of the ghost peaks. A semi-quantitative analysis can be made. This is accomplished in two steps, first by considering a first-principles physical model for the photoelectron current in an XPS experiment. As described by Powell [9], the detected XPS photoelectron current I_s (from level X of species i in the sample) can be written as

$$I_s(E_{i,X}) = I(\hbar\omega)N_i\sigma_i(\hbar\omega,\theta,X)\lambda_s(E_i)F(E_i,E_a)T(E_i,E_a)D(E_a)G_A \quad (1)$$

where I is the photon flux, N_i is the species concentration, σ_i is the differential photoionization cross-section, λ_s is the total inelastic mean free path,

F is an analyzer optical factor, T is the analyzer transmission function, D is the detector efficiency, and G_A is a geometrical factor for the experiment. We can calculate the ratio of O $K\alpha$ to Mg $K\alpha$ photon fluxes incident on the sample by considering the Au $4f_{7/2}$ signals from Au foil caused by O $K\alpha$ or Mg $K\alpha$ excitation. For simplicity we retain only an O or Mg subscript on each term in eqn (1) denoting the excitation. The factors N_1 , D , and G_A are independent of photon energy and can be ignored in the ratio. The photoionization cross-section for orbitals that can be ionized by O $K\alpha$ photons is much larger for O $K\alpha$ than for Mg $K\alpha$ excitation [10]. While the Au $4f_{7/2}$ photoionization cross-sections at the O $K\alpha$ and Mg $K\alpha$ photon energies are not known experimentally, theoretical calculations suggest $\sigma_{\text{O}}/\sigma_{\text{Mg}} \approx 8.5$ [11]. The mean free path of the lower-kinetic-energy photoelectrons is shorter, and $\lambda_{\text{O}}/\lambda_{\text{Mg}} = 0.47$, using a calculation suggested by Penn [12]. The analyzer luminosity $L = F \times T$ is such that $L \propto 1/E_1$ for a cylindrical-mirror analyzer operated in the retarding mode. Thus $F_{\text{O}} T_{\text{O}}/F_{\text{Mg}} T_{\text{Mg}} = 2.65$. We can substitute the measured relative intensity of the ghost peak ($I_{s,\text{O}}/I_{s,\text{Mg}} \approx 0.11$) and determine the relative flux of O $K\alpha$ and Mg $K\alpha$ photons incident on the sample as $I_{\text{O}}/I_{\text{Mg}} \approx 0.010$.

The second step is to connect the relative O $K\alpha$ photon flux at the sample to the amount of oxygen impurity in the Mg anode. The $K\alpha$ photon flux I (photons steradian⁻¹ s⁻¹) emerging from the source is

$$I = I_e(1/4\pi)N_\phi T \quad (2)$$

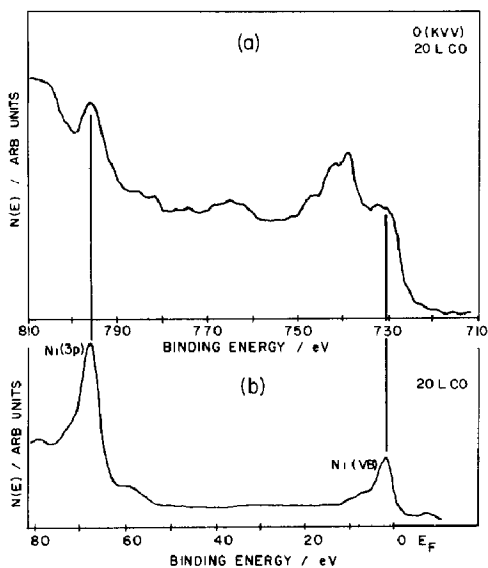


Fig 3 (a) XAES O(KVV) spectrum of 20 L CO on Ni(100) at 300 K obtained using an oxidized Mg anode. The spectrum contains significant contributions from O $K\alpha$ ghost photoelectron peaks of Ni 3p and Ni VB (= valence band) (b) The Ni 3p and Ni VB photoelectron peaks due to Mg $K\alpha$ excitation

where I_e is the electron current impinging on the anode at electron kinetic energy T_0 from the filament, N_ϕ is the number of $K\alpha$ photons emitted at an angle ϕ with respect to the anode surface for each incident electron, and T is the transmission of the 2- μm Al window at the end of the source. We can calculate the concentration ratio of O to Mg atoms in the anode by inserting the previously determined photon flux ratio I_O/I_{Mg} from eqn (1) and evaluating the factors in eqn (2) for both O $K\alpha$ and Mg $K\alpha$ emission, identified by O and Mg subscripts. Our method requires a calculation of the photon yield upon electron bombardment of a thick target composed of O and Mg atoms. Assuming the oxygen impurity to be in the form MgO and present in the near-surface layers, we can calculate the oxide thickness required to give the calculated relative O $K\alpha$ flux.

The primary-electron current I_e and the geometric factor $1/4\pi$ cancel in the ratio. The 2- μm Al window at the end of the source greatly attenuates low-energy radiation, and $T_O/T_{Mg} = 0.037/0.699 = 0.0529$ [13]. N_ϕ is given [14] by

$$N_\phi = k \int_{T_0}^{E_K} \exp(-(\mu/\rho)\rho \operatorname{cosec} \phi) \frac{\partial n}{\partial x} \frac{\partial x}{\partial T} dT \quad (3)$$

where T is the electron kinetic energy, T_0 the incident energy, and E_K the K -shell ionization energy. The factor k relates the observed photon intensity to the number of primary-ionization events. The exponential term accounts for self-absorption by the anode of radiation traveling a distance $x \operatorname{cosec} \phi$ in material of density ρ and mass attenuation coefficient μ/ρ . The term $\partial n/\partial x$ relates the number of K -ionizations n per electron and the depth of electron penetration x , and $\partial n/\partial x = NQ$ where N is the density of atoms producing $K\alpha$ photons and Q is the total K -ionization cross-section. Since Q is a function of electron energy, we need to know the relation $\partial x/\partial T$ between the electron kinetic energy and depth of penetration. Before we evaluate the integral in eqn (3), we calculate k .

The factor k [15] given by

$$k = pwR(P + 1)/P \quad (4)$$

allows for (a) indirect production of $K\alpha$ photons by photoexcitation of K shells by the continuous radiation (bremsstrahlung), where P is the ratio of directly to indirectly produced K ionizations, (b) fluorescence yield w , (c) the ratio p of the number of $K\alpha$ photons to total K photons produced, and (d) electron re-diffusion R . Known line-intensities give $p_O/p_{Mg} = 1.00/0.88 = 1.1$. Fluorescence yields for light atoms in condensed matter give $w_O/w_{Mg} = 0.0058/0.028 = 0.0529$, but chemical effects significantly change these values so that the uncertainty is between 10 and 40% [16]. Indirectly produced K ionization is important, but since the photoionization cross-section is sharply peaked we can make the simplifying assumption $[(P_O + 1)/P_O]/$

$[(P_{\text{Mg}} + 1)/P_{\text{Mg}}] \approx 1$ We also set $R_{\text{O}}/R_{\text{Mg}} \approx 1$ This gives $k_{\text{O}}/k_{\text{Mg}} = 0.0058/0.025 = 0.24$ Substituting the numbers we have so far into eqn (2), we find that the ratio for the integral given in eqn (3), evaluated for O and Mg K ionization, is required to take the value 0.79 to account for $I_{\text{O}}/I_{\text{Mg}} = 0.010$ We now proceed to the numerical integration

The source geometry is such that $\phi = 90^\circ$ and $\text{cosec } \phi = 1$, and the primary electrons strike the anode near normal to the surface Values for the K-ionization cross-section Q can be found [17] by using

$$Q_K = 7.92 \times 10^{-20} (C_K/TE_K) \ln(T/E_K) \quad [\text{cm}^2] \quad (5)$$

in which $C_K = 0.85 + 0.0047Z$, where Z is the atomic number, and T and E_K are in keV The relativistic electron stopping-power of a homogeneous, multi-element material can be given [18] by

$$\begin{aligned} (1/\rho)dT/dx = & (3.076 \times 10^2/\beta^2) \sum_i C_i(Z_i/A_i) \{ \ln(T/J_i) \sqrt{\gamma+1} + 0.153 \\ & - (\beta^2/2) + (1/16)[(\gamma-1)/\gamma]^2 - (0.693)(2\gamma-1)/2\gamma^2 \} \\ & [\text{keV cm}^2 \text{g}^{-1}] \quad (6) \end{aligned}$$

where the summation is over all elements i in the material, T is in keV and x is in cm, ρ is the density of the material in g cm^{-3} , and where C_i , Z_i , A_i , and J_i are respectively the weight fraction, atomic number, atomic weight, and average ionization energy of element i The solution of a simple non-relativistic electron stopping-power expression [14] can be used to determine the penetration depth for a given energy according to

$$x = 3.176 \times 10^{-6} (J^2 A / \rho Z) [E_i(2\alpha_0) - E_i(2\alpha)] \quad [\text{cm}] \quad (7)$$

where J and T are in keV, and $\alpha_0 = \ln(2T_0/J)$ and $\alpha = \ln(2T/J)$ This formula can be modified as in eqn (6) for a multi-element material. The integration in eqn (3) can be carried out for O and Mg K ionization with an arbitrary thickness of MgO at the anode surface, by using the appropriate O and Mg atom densities, etc., in MgO, and then continued for Mg K ionization in pure Mg to the point $T = E_K$ We found that a surface MgO layer of thickness $0.26 \mu\text{m}$ would account for the observed Au 4f O K α relative intensity The range (average path length), including the MgO layer, for the 10-keV primary electrons to slow to $E_K(\text{Mg})$ was $1.3 \mu\text{m}$.

The results of this calculation indicate substantial oxidation of the Mg anode, but this is plausible At room temperature, Mg forms a protective MgO film $\sim 70 \text{ \AA}$ thick However, the thicker oxide films formed at higher temperatures ($>450^\circ\text{C}$) result in a loss of the protective nature of the oxide The surface of the Mg anode during operation of the X-ray source is under bombardment by 10-kV electrons dissipating 400 W of energy at the anode surface The local heating of the anode surface that occurs, in addition to the effects of the large charge-flow that takes place through the anode, could

allow for the formation of an oxide film of the order of 2000 Å thick. There is some empirical evidence for the formation of oxide layers of this thickness on used Mg anodes. A depth profile obtained by sputtering and AES of an oxidized Mg anode gave the following results [19]: surface, 33% O, -120 Å, 40% O, -240 Å, 40% O, -350 Å, 48% O, -600 Å, 24% O, -1000 Å, 7% O, where the percentage of oxygen given is in atomic percent and only the elements Mg and O were detected. Importantly, depth profile results on a new Mg anode indicate a much smaller, but significant, oxide level at -150 Å [19]. Our conclusion is that there is no physical basis to rule out a significant O $K\alpha$ emission intensity from an oxidized Mg anode, even at a much lower oxide level than for the anode discussed above (Au 4f O $K\alpha$ ghost of ~11% relative intensity). Similar arguments can be made in regard to O $K\alpha$ emission intensity from an oxidized Al anode. Calculations show that an oxide layer on the 2- μ m Al window would not contribute to a significant O $K\alpha$ emission intensity from the source.

In studying chemisorbed species using XAES, the presence of even a very small amount of O $K\alpha$ intensity is important, due to the large intensity-differences between the substrate photoelectron peaks and the adsorbate Auger features. For carbon, oxygen, and nitrogen XAES spectra, consideration must be given to possible O $K\alpha$ ghosts from photoelectron peaks in the BE regions 330–230, 80–0, and 190–90 eV, respectively. Notably, there are two cases where ghost peaks will interfere for any system if O $K\alpha$ intensity is present: (1) the C 1s ghost appears in the C(KVV) spectra, and (2) the substrate valence-band ghost appears in the O(KVV) spectra. One of the clearest means for detecting and calibrating the relative intensities of these ghosts is through the use of a clean Au standard sample as demonstrated here.

REFERENCES

- 1 P H Holloway, T E Madey, C T Campbell, R R Rye and J E Houston, *Surf Sci*, 88 (1979) 121
- 2 M S Bana and D A Shirley, *J Chem Phys*, 63 (1975) 4759
- 3 S Evans and E Raftery, *J Electron Spectrosc Relat Phenom*, 17 (1979) 137
- 4 C D Wagner, W M Riggs, L E Davis and J F Moulder, in G E Muilenberg (Ed), *Handbook of X-ray Photoelectron Spectroscopy*, Perkin-Elmer Corporation, Eden Prairie, MN, 1979, p 13
- 5 E N Sickafus, *Rev Sci Instrum*, 42 (1971) 933
- 6 H H Madden and J E Houston, *Adv X-ray Anal*, 19 (1976) 657
- 7 H H Madden and J E Houston, *J Appl Phys*, 47 (1976) 3071
- 8 R R Rye, J E Houston, D R Jennison, T E Madey and P H Holloway, *Ind Eng Chem, Prod Res Dev*, 18 (1979) 18
- 9 C J Powell, in N S McIntyre (Ed), *ASTM STP 643*, American Society for Testing and Materials, 1978, pp 5–30
- 10 J Berkowitz, *Photoabsorption, Photoionization, and Photoelectron Spectroscopy*, Academic Press, New York, 1979, p 155

- 11 J H Scofield, Lawrence Livermore Lab Rep , UCRL-51326, 1973
- 12 D R Penn, J Electron Spectrosc Relat Phenom , 9 (1976) 29
- 13 W J Vegele, in J W Robinson (Ed), Handbook of Spectroscopy, Vol 1, CRC Press, Cleveland, OH, 1974, p 155
- 14 L R Worthington and S G Tomlin, Proc Phys Soc London, Sect A, 69 (1956) 401
- 15 P Kirkpatrick and A V Baez, Phys Rev , 71 (1947) 521
- 16 M O Krause, J Phys Chem Ref Data, 8 (1979) 307
- 17 D B Brown, in J W Robinson (Ed), Handbook of Spectroscopy, Vol 1, CRC Press, Cleveland, OH, 1974, p 248
- 18 D B Brown, in J W Robinson (Ed), Handbook of Spectroscopy, Vol 1, CRC Press, Cleveland, OH, 1974, p 249
- 19 T Rusch, Perkin—Elmer, Physical Electronics Division, Eden Prairie, MN, personal communication